

# Synthesis of Rubidium-doped Calcium Hydroxyapatite Nanoparticles for Biomedical Applications

<sup>a</sup>Awais Nisar<sup>1</sup>, <sup>a</sup>Sajid Iqbal, <sup>a</sup>Mohsin Ali Raza Anjum, <sup>b</sup>Munib Ahmed Shafique, <sup>c</sup>Syed Zahid Hussain, <sup>c</sup>Qanita Ttayyaba

<sup>a</sup> Chemistry Division, PINSTECH, P.O. Nilore, Islamabad 45650, Pakistan

<sup>b</sup> Central Analytical Facility Division, PINSTECH, P.O. Nilore, Islamabad 45650, Pakistan

<sup>c</sup> Material Division, PINSTECH, P.O. Nilore, Islamabad 45650, Pakistan

\*Corresponding Author: sajid1@alumni.kiast.ac.kr

## Abstract

Due to high biocompatibility, bioactivity, and natural occurrence in bones and teeth, synthetic calcium hydroxyapatite (Ca-HAp) is a widely applied biomaterial in tissue engineering, including orthopedic surgery and dentistry. However, the brittle nature and low strength reduce its durability, which can be improved by doping metal ions. Rubidium (Rb) is an essential trace element that works as an antibacterial agent in the human body; therefore, it can be doped in synthetic Ca-HAp to promote its durability. In this work, Rb-doped calcium hydroxyapatite (Rb-HAp) nanoparticles are synthesized by the co-precipitation method at low temperatures. Phase purity, crystallinity, doping level, and mechanical properties are investigated by X-ray diffraction (XRD), inductively coupled plasma optical emission spectroscopy (ICP-OES), and micro-hardness tester. It is observed that a minute quantity ( $\approx 0.02\%$ ) of Rb remained in the apatite structure when 5% of Rb<sup>+</sup> is doped via in situ method. Moreover, small dopant concentration did not affect the crystal structure and the tensile strength of HAp.

**Keywords:** Hydroxyapatite, Doping, Mechanical properties, Biomedical.

## Introduction

With the rise in skeletal injuries and teeth implantation due to the increasing number of accidents and trauma cases, there is a dire need to develop biocompatible, bioactive, safe, and osteoconductive biomaterial that can fill the bone defects or replace the broken skeletal part within the body [1]. With the rapid advancement in nanoscience and nanobiotechnology, synthetic polymeric materials (e.g., polyethylene, polyurethane foam & polylactic acid) are commonly used as medical implants instead of expensive metal-based implant materials their biological stability. Also, they do not produce microwaves or electrolytic current in metallic implants [2]. However, many challenges are associated with polymeric implants such as material biocompatibility, osteointegration, poor mechanical properties, and adverse immunologic reactions [2]. The natural bone consists of calcium phosphate minerals. Advanced microscopic analysis of bone and teeth revealed that they are naturally constructed by calcium hydroxyapatite (Ca-HAp) stacked in the form of fibrils [3]. The low ductility and brittle nature of synthetic HAp are the main obstacles in using these implants. However, its durability and biocompatibility have been enhanced by developing polymeric composites, e.g., Silk fibroin/hydroxyapatite [4], hydroxyapatite-doped polycaprolactone nanofibers [5], polylactic acid/hydroxyapatite [6], hydroxyapatite-natural polymers nanocomposites, etc. [7]. Similarly, natural bone-like properties can be achieved by doping several metallic/nonmetallic species such as Na<sup>+</sup>, Fe<sup>2+/3+</sup>, Mg<sup>2+</sup>, Co<sup>2+</sup>, Ag<sup>+</sup>, Sr<sup>2+</sup>, Cl<sup>-</sup>, CO<sub>3</sub><sup>2-</sup>, SiO<sub>4</sub><sup>2-</sup> etc. into the crystal structure of Ca-HAp [8]. Due to the high ion exchange capability of pristine Ca-HAp, the desired metal cations or anions can be easily doped to get appropriate hardness, compressive strength, and biocompatibility [9].

The primary cause of implantation failure is bacterial infection after the implant replacement. It is well-known that the traditional treatment (i.e., mechanical debridement) of bacterial inflammation with antibiotics and

antibacterial agents has certain limitations [10]. Therefore, scientists and researchers are trying to develop biomaterials having intrinsic antibacterial capacity. It is reported that the antibiotic, antifungal, and antimicrobial properties can be created in the HAp structure by doping certain elements like Ag<sup>+</sup>, Cu<sup>2+</sup> or Zn<sup>2+</sup>, etc. [11-14].

Rubidium (Rb) is an essential trace element that accelerates the growth of animals and plants. It also acts as an antibacterial and skin wound healing agent, especially in diabetic patients [15]. Rb physiologically resembles potassium and it is present virtually in all living systems. Spectrographic analysis revealed that Rb<sup>+</sup> is present in the dry weight range of  $2 \times 10^{-3}$  to  $6 \times 10^{-8}$  % in all animal tissues [16]. Rb metal is vital for behavioral pharmacology and electrolyte physiology [17]. Recently, Rb has been considered a suitable candidate for doping in HAp as it has revealed an improved cytocompatibility [15]. The prepared Rb-doped implant material also showed a higher inhibition against bacteria. Tan et al. [12] studied the influence of Rb on HAp phase composition, microstructure, mechanical properties, and cell response of bioactive glass-ceramics intended to use for biomedical applications. Their results also showed enhanced bioactivity and biocompatibility of Rb-doped HAp (Rb-HAp), thus making it a suitable candidate for biomedical applications. In-vitro studies of Rb-HAp showed a better proliferation and differentiation of MG-63 cells and showed bacterial inhibition towards E.Coli and S. Aureus (ATCC 8739, ATCC 6538) [18].

This study is designed to incorporate Rb<sup>+</sup> in the HAp matrix to enhance the efficiency of bone and teeth implants without losing their biocompatibility and mechanical properties.

## Materials and Methods

All chemicals used for the synthesis of nanomaterials were purchased from Sigma Aldrich and used without further purifications. Pure and doped samples of Ca-HAp were prepared by the wet precipitation method [19]. Briefly, 1.28 M aqueous solution of diammonium hydrogen phosphate (DAHP, Merck) and 0.75 M calcium nitrate tetrahydrate



(Ca(NO<sub>3</sub>)<sub>2</sub>·4H<sub>2</sub>O) were prepared in 100 ml of deionized water. To prepare the Rb-doped HAp nano-bio material, the stoichiometric amount of rubidium chloride (RbCl, Merck) was dissolved in a calcium nitrate aqueous solution. The concentrations of Ca(NO<sub>3</sub>)<sub>2</sub>·4H<sub>2</sub>O and DAHP solutions are adjusted with the introduction of RbCl in the metal solution to keep the (Ca+Rb)/P molar ratio to 1.67. A stoichiometric amount of DAHP solution was added gradually from the burette to the metal salt solution (Ca and Rb) which was kept at 40°C on a hot plate. To main the accuracy of temperature, an external mercury thermometer was also used. The pH of the reaction was adjusted with the help of aqueous ammonia (NH<sub>4</sub>OH) solution and maintained throughout the reaction at 10.4 with the help of calibrated pH meter (Metrohm, Model-827). The reaction mixture was stirred for 1.5 h approximately and then aged at 40 °C for 24 h. After that, the supernatant was decanted and precipitates were collected, washed five times with distilled water, and separated by centrifugation at 4000 RPM. The obtained crystals were dried at 100 °C in a drying oven for 24 h. The obtained dried crystals were pulverized to form a fine powder and stored in a desiccator for further characterizations. X-ray diffraction (XRD) patterns of the pure HAp and Rb-doped HAp (1-5 wt. %) were obtained by a diffractometer (RIGAKU, Japan).

The as-synthesized powder was digested in 0.1 M HNO<sub>3</sub> to estimate the Rb contents using an inductively coupled plasma optical emission spectrometer (ICP-OES, Thermo scientific iCAP 6000). To determine mechanical properties, the sample pellets were prepared by uniaxial compression on a 2.5 MPa load using a uniaxial press machine. Then these pellets were sintered at a temperature of 1300 °C in a muffle furnace for 2 h with a heating ramp of 3°C/min. To estimate the yield stress and tensile strength of sintered pellets, the micro-hardness was determined using Vickers micro-hardness indenter (MATSUZAWA SEIKI Co, LTD, Japan). Before each measurement, compact cylinders were first mounted using epoxy molds for efficient results. The pellet's surface was smoothed using a range of grit size papers (800 to 2000). The surface was further polished with the help of fine cloth using 1µm diamond paste. The average value of ten indentations was taken for each data point.

Vickers hardness (VH) was calculated by using Equation 1 [20].

$$HV = 0.001854 \frac{P}{d^2} \quad (1)$$

HV is Vickers hardness in GPa, P is the applied load (500 g or 4.9 N), and d is diagonal indent length (mm).

## Results and discussion

ICP-OES measured the concentration of Rb<sup>+</sup> in all doped samples. Rb<sup>+</sup> was not detected in 1, 2, 3 and 4 % Rb-HAp samples. However, in the 5 % Rb-HAp sample, only 8.37 ppm (0.02%) was found, which confirmed the loading of Rb<sup>+</sup> ions into the HAp structure. Therefore, it is expected that the physicochemical and mechanical properties of HAp will be changed despite the low doped concentration of Rb [13, 21-24].

Figure 1 shows the XRD patterns of pure and Rb-HAp samples. According to JCPDS card No: 00-009-0432, a phase pure HAp is successfully formed with an average crystallite size of 60 nm. As expected, no significant alteration in the crystal structure of HAp was observed after the loading of Rb<sup>+</sup> ions. The absence of Rb<sup>+</sup> peaks may be due to the small loading of Rb metal ions (0.02 %). HAp main peaks have retained their peak position and peak width. Again, this is due to the doping of a minute number of Rb<sup>+</sup> ions at the interstitial sites of HAp crystals or the replacement of its Ca<sup>2+</sup>/H<sup>+</sup> cations. This confirms that the apatite lattice remained intact after the successful doping of metal in the apatite structure.

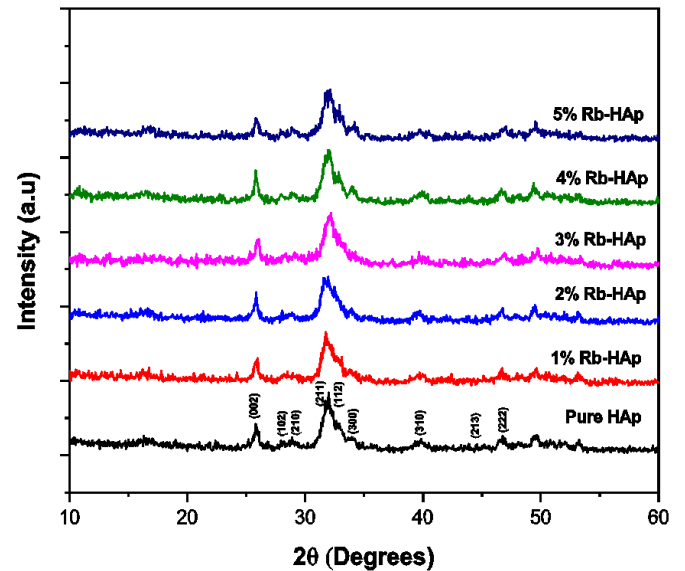


**Figure 1: XRD patterns of pure HAp and Rb doped HAp samples**

The stoichiometric composition of HAp has a hexagonal structure with a P6<sub>3</sub>/m space group with lattice parameters of a=b=9.43 Å and c=6.88 Å. The two distinct sites of Ca<sup>2+</sup> ions in the unit cell are Ca(I) and Ca(II) sites [25]. It may be hypothesized that the dopant ion larger than the Ca<sup>2+</sup> ion would substitute the Ca(I) site present in the apatite structure and the smaller one would go for the Ca(II) site [26]. It is reported that the preference of the substitution site depends on the effective charge of foreign metal ions [27]. If the foreign ion has an effective charge smaller than that of Ca<sup>2+</sup>, it will occupy a larger site, i.e., Ca(I) and vice versa [27]. Keeping in view the above investigations, it is expected that the Rb<sup>+</sup> ion will replace the Ca(I) site. During the replacement process, either the Rb<sup>+</sup> ion will cause a vacancy in HAp or the charge is balanced with the eventual loss of H<sup>+</sup> from the apatite structure [28]. If the vacancy is generated in the HAp structure, it may improve the electrical properties of bone as electric fields are thought to have positive effects on bone healing [29].

To determine the mechanical strength, the micro-hardness was determined and the results are summarized in Table 1. It is observed that the hardness of Rb-HAp did not deteriorate. The values of hardness and estimated tensile strength are better than the natural hardness and tensile strength of

human bone. The hardness and tensile strength of human bone depend upon the type of bone, age group, and gender. For example, in the case of a male, the mean ultimate tensile strength of bone is in the range of 7.28 kg/mm<sup>2</sup> (0.07 GPa) to 9.99 kg/mm<sup>2</sup> (0.09 GPa) [30]. Considering these values, the prepared scaffold is better in ultimate tensile strength than that of natural bone.

The hardness value of human dry bone is 35 HV (0.343 GPa), while it is 10 % less in the case of wet bone [31]. For both cases, our material meets the mechanical properties of the implant. Hence, Rb-doped HAp nanomaterials can be employed as a reliable antibacterial implant or replace the defective teeth and bone structures as reported in the literature [1, 11, 12, 15].

**Table 1. Hardness and tensile strength of pure and doped HAp samples**

Doping concentration	Hardness (GPa)	Estimated Tensile Strength (GPa)
Pure HAp	4.40 ± 0.5	1.45 ± 0.5
0.02 % Rb-HAp	4.29 ± 0.4	1.50 ± 0.4

### Conclusions

The pure and Rb-doped HAp samples were synthesized and characterized by XRD, ICP-OES for biomedical applications. It was found that Rb<sup>+</sup> ions hardly replace Ca<sup>2+</sup> ions in the structure of HAp. Rb was successfully replaced Ca<sup>2+</sup> in HAp and did not alter HAp crystal structure by increasing the weight percent of dopant. The micro-hardness testing revealed no degradation in the hardness of the prepared pellet. The obtained hardness and tensile strength are much better than the natural mechanical properties of human bone. Therefore, Rb may be a suitable candidate for biomedical applications due to its good mechanical properties.

### Acknowledgments

We are thankful to the Pakistan Institute of Nuclear Science and Technology (PINSTECH) for supporting this work.

### References

- Liu, Y., Y. Tan, and J. Wu, *Rubidium doped nano-hydroxyapatite with cytocompatibility and antibacterial*. Journal of Asian Ceramic Societies, 2021: p. 1-11.
- Saini, M., et al., *Implant biomaterials: A comprehensive review*. World Journal of Clinical Cases: WJCC, 2015. **3**(1): p. 52.
- Bostancioglu, R.B., et al., *Adhesion profile and differentiation capacity of human adipose tissue derived mesenchymal stem cells grown on metal ion (Zn, Ag and Cu) doped hydroxyapatite nano-coated surfaces*. Colloids and Surfaces B: Biointerfaces, 2017. **155**: p. 415-428.
- Farokhi, M., et al., *Silk fibroin/hydroxyapatite composites for bone tissue engineering*. Biotechnology advances, 2018. **36**(1): p. 68-91.
- Han, F., et al., *Hydroxyapatite-doped polycaprolactone nanofiber membrane improves tendon–bone interface healing for anterior cruciate ligament reconstruction*. International journal of nanomedicine, 2015. **10**: p. 7333.
- Alksne, M., et al., *In vitro comparison of 3D printed poly(lactic acid)/hydroxyapatite and poly(lactic acid)/bioglass composite scaffolds: Insights into materials for bone regeneration*. Journal of the mechanical behavior of biomedical materials, 2020. **104**: p. 103641.
- Chung, J.-H., et al., *Synthesis, characterization, biocompatibility of hydroxyapatite–natural polymers nanocomposites for dentistry applications*. Artificial cells, nanomedicine, and biotechnology, 2016. **44**(1): p. 277-284.
- Wopenka, B. and J.D. Pasteris, *A mineralogical perspective on the apatite in bone*. Materials Science and Engineering: C, 2005. **25**(2): p. 131-143.
- Cawthray, J.F., et al., *Ion exchange in hydroxyapatite with lanthanides*. Inorganic chemistry, 2015. **54**(4): p. 1440-1445.
- Li, X., et al., *Surface treatments on titanium implants via nanostructured ceria for antibacterial and anti-inflammatory capabilities*. Acta biomaterialia, 2019. **94**: p. 627-643.
- Ahmed, M., et al., *Physical and biological changes associated with the doping of carbonated hydroxyapatite/polycaprolactone core-shell nanofibers dually, with rubidium and selenite*. Journal of Materials Research and Technology, 2020. **9**(3): p. 3710-3723.
- Tan, Y.-n., et al., *Rubidium-modified bioactive glass-ceramics with hydroxyapatite crystals for bone regeneration*. Transactions of Nonferrous Metals Society of China, 2021. **31**(2): p. 521-532.
- Stanić, V., et al., *Synthesis of antimicrobial monophase silver-doped hydroxyapatite nanopowders for bone tissue engineering*. Applied Surface Science, 2011. **257**(9): p. 4510-4518.
- Zamperini, C., et al., *Antifungal applications of Ag-decorated hydroxyapatite nanoparticles*. Journal of Nanomaterials, 2013. **2013**.
- He, X., et al., *Rubidium-containing calcium alginate hydrogel for antibacterial and diabetic skin wound healing applications*. ACS biomaterials science & engineering, 2019. **5**(9): p. 4726-4738.
- Relman, A.S., *The physiological behavior of rubidium and cesium in relation to that of potassium*. The Yale journal of biology and medicine, 1956. **29**(3): p. 248.
- Fieve, R.R., et al., *Rubidium: biochemical, behavioral, and metabolic studies in humans*. American Journal of Psychiatry, 1973. **130**(1): p. 55-61.
- Liu, Y., Y. Tan, and J. Wu, *Rubidium doped nano-hydroxyapatite with cytocompatibility and antibacterial*. Journal of Asian Ceramic Societies, 2021. **9**(1): p. 323-333.
- Cahyaningrum, S., et al. *Synthesis and characterization of hydroxyapatite powder by wet precipitation method*. in *IOP Conference Series: Materials Science and Engineering*. 2018. IOP Publishing.
- Uysal, I., F. Severcan, and Z. Evis, *Structural and mechanical characteristics of nanohydroxyapatite*

- doped with zinc and chloride*. *Advances in Applied Ceramics*, 2013. **112**(3): p. 149-157.
21. Padmanabhan, V.P., et al., *Facile fabrication of phase transformed cerium (IV) doped hydroxyapatite for biomedical applications—A health care approach*. *Ceramics International*, 2020. **46**(2): p. 2510-2522.
  22. Barinoy, S., et al., *Stabilization of carbonate hydroxyapatite by isomorphic substitutions of sodium for calcium*. *Russian Journal of Inorganic Chemistry*, 2008. **53**(2): p. 164-168.
  23. Shi, C., et al., *Ultra-trace silver-doped hydroxyapatite with non-cytotoxicity and effective antibacterial activity*. *Materials Science and Engineering: C*, 2015. **55**: p. 497-505.
  24. Korbas, M., et al., *Bone tissue incorporates in vitro gallium with a local structure similar to gallium-doped brushite*. *JBIC Journal of Biological Inorganic Chemistry*, 2004. **9**(1): p. 67-76.
  25. Wang, M., et al., *Computer simulation of ions doped hydroxyapatite: a brief review*. *Journal of Wuhan University of Technology-Mater. Sci. Ed.*, 2017. **32**(4): p. 978-987.
  26. Ciobanu, G., A.M. Bargan, and C. Luca, *New cerium (IV)-substituted hydroxyapatite nanoparticles: Preparation and characterization*. *Ceramics International*, 2015. **41**(9): p. 12192-12201.
  27. Getman, E., et al., *Substitution of samarium for strontium in the structure of hydroxyapatite*. *Functional materials*, 2011.
  28. Tite, T., et al., *Cationic substitutions in hydroxyapatite: Current status of the derived biofunctional effects and their in vitro interrogation methods*. *Materials*, 2018. **11**(11): p. 2081.
  29. Gittings, J., et al., *Electrical characterization of hydroxyapatite-based bioceramics*. *Acta Biomaterialia*, 2009. **5**(2): p. 743-754.
  30. Wall, J., S. Chatterji, and J. Jeffery, *Age-related changes in the density and tensile strength of human femoral cortical bone*. *Calcified tissue international*, 1979. **27**(1): p. 105-108.
  31. Dall'Ara, E., et al., *The effect of tissue condition and applied load on Vickers hardness of human trabecular bone*. *Journal of biomechanics*, 2007. **40**(14): p. 3267-3270.



Creative Commons License

This work is licensed under a Creative Commons Attribution 4.0 International License.